

# RSC Advances



This is an *Accepted Manuscript*, which has been through the Royal Society of Chemistry peer review process and has been accepted for publication.

*Accepted Manuscripts* are published online shortly after acceptance, before technical editing, formatting and proof reading. Using this free service, authors can make their results available to the community, in citable form, before we publish the edited article. This *Accepted Manuscript* will be replaced by the edited, formatted and paginated article as soon as this is available.

You can find more information about *Accepted Manuscripts* in the [Information for Authors](#).

Please note that technical editing may introduce minor changes to the text and/or graphics, which may alter content. The journal's standard [Terms & Conditions](#) and the [Ethical guidelines](#) still apply. In no event shall the Royal Society of Chemistry be held responsible for any errors or omissions in this *Accepted Manuscript* or any consequences arising from the use of any information it contains.

Cite this: DOI: 10.1039/c0xx00000x

www.rsc.org/xxxxxx

ARTICLE TYPE

# Enhancement on electrochemical performance of silicon nanowires by homostructured interface used as anode materials for lithium ion batteries

Zhongsheng Wen,<sup>\*a</sup> Zhongyuan Zhang<sup>a</sup> and Guanqin Wang<sup>a</sup>

<sup>5</sup> Received (in XXX, XXX) Xth XXXXXXXXX 20XX, Accepted Xth XXXXXXXXX 20XX  
DOI: 10.1039/b000000x

A novel and facile approach to fabricating long life silicon nanowires (SiNWs) via interface enhancement by structuring silicon interface between SiNWs and metallic substrates from nonequilibrium Si-Au composite based on conventional vapor-liquid-solid mechanism is successfully demonstrated in the paper. The building of Si transition layer as an interface successfully converts the interface contact of SiNWs on the substrates from point contact between SiNWs and stainless steel substrate into planar contact between Si film and stainless steel substrate. Although the interface modification process is very simple, the improved high stability of SiNWs by this way proves that it is a very promising strategy to get long life for high capacity anode materials used in lithium ion batteries. The building of silicon homo-structural interface between assembled SiNWs and metallic substrates results in ultra long life for SiNWs. The retention capacity of produced SiNWs is up to 2447mAh g<sup>-1</sup> even after 100 cycles, delivering 80.92% of its second discharge capacity, presenting a very attractive cycling stability.

## Introduction

Fossil energy crisis and environmental issues facilitate the development of green transportation devices. Rechargeable lithium-ion batteries are the most attractive power sources for environment friendly electric vehicles and hybrid electric vehicles because of their excellent performance over any other conventional batteries. Safety, high energy density and long cyclability are the indispensable factors for lithium ion batteries to be applied successfully in these fields. From a material standpoint, intense worldwide efforts have been devoted to seek superior electrode materials<sup>1, 2</sup> to substitute the current commercialized lithium transition oxides/graphite electrode system, whose specific capacities constrain the overall energy density of lithium ion batteries. Although suffering from the poor cyclability triggered by high volume changes,<sup>3</sup> which is induced by lithium insertion into and the subsequent extraction from the crystal lattice of silicon, silicon anode material is still attractive for its high theoretic specific capacity (4200mAh g<sup>-1</sup>, ten times of the commercialized graphite anode materials) as well as suitable voltage plateau.

Decreasing the size of silicon active material has been demonstrated feasible to alleviate the structural collapse caused by contrast volume changes. One dimensional silicon, e. g. silicon nanowires (SiNWs) or silicon nanotubes, has been proved to possess high mechanical intensity along longitude to resist against the volume stress caused by lithium insertion and extraction.<sup>4-6</sup> Bottom-up method by the aid of metal catalysts based on Vapor-Liquid-Solid (VLS) mechanism is a conventional

way to synthesize SiNWs, in which metal catalysts generally alloy with silicon to form eutectic alloy to provide the circumstances for the nucleation of silicon seeds.<sup>7-10</sup> Au is a preferable catalyst for SiNW growth because Si and Au can form Si-Au eutectic alloy at a relatively low temperature of 368 °C as well as high Si solubility of 12% in this intermediate eutectic.<sup>6</sup> Although volume expansion on longitude direction is constrained well to a low extent during lithium insertion and extraction, however, the expansion on radical direction could not be eliminated, which is still up to ca. 300% of its pristine size after lithium insertion.<sup>5</sup> An interesting phenomenon should be noted. It is very hard to obtain a long life for SiNWs despite many references demonstrated the structural stability of SiNWs during electrochemical lithium insertion and extraction, although there was almost no fracture found in SiNWs.<sup>6, 9-11</sup>

Some insight research was conducted to elucidate the reason of the unpromising cycling life in our group. In our pervious study, we found the disconnection occurred essentially between the substrates and SiNWs when we opened the batteries after deep depth cycling. Metals with stable property in electrolyte is preferred as the current collector in lithium ion batteries, so stainless steel and nickel foil are always chosen as the substrate for SiNW growth, considering their good thermal resistance and stable chemical performance in organic electrolyte for lithium ion batterie, so we deduced that the interface between the metallic substrate and SiNWs is very weak, which should be induced by the crystal lattice mismatch between deposited SiNWs and their substrates, therefore interface de-bonding behavior would likely take place when serious expansion-shrinkage in volume occurs

during correspondingly electrochemical lithium insertion-extraction.

Relatively shallow depth by limiting the lithium inserting voltage to a higher cutoff range is a feasible way to alleviate the disconnection in interface.<sup>6, 10</sup> Surface modification via depositing carbon layer around SiNWs or microstructure modification via architecting core-shell microstructure, in which the inert core or inert coating film acts as the scaffold of the active center to support stable mechanical structure and fine electrical connection, is proved feasible to improve the cycling performance of SiNWs.<sup>11-16</sup> Another promising way is to increase the contacting area between substrates and active silicon centre, which has been demonstrated efficient in silicon film prepared on metal substrates.<sup>2, 11, 16-18</sup> These surface modification, fabrication of carbon matrix composite were the conventional way to modify these high capacity materials, and many reports also demonstrated the feasibility of these methods. However, the interface issues are almost ignored, and have never been noted and mentioned in most of the previous reports.

Our exploration found that fabricating suitable interface could be most effective way to realize the life stability of SiNWs. In this paper, A novel and facile approach to fabricating long life silicon nanowires (SiNWs) via interface enhancement by homostructured interface between SiNWs and metallic substrates from nonequilibrium Si-Au composite catalyst is successfully demonstrated in the paper. Although the interface modification process is very simple, the improved high stability of SiNWs by this way proves that it is a very promising strategy to get long life anode materials with high capacity for lithium ion batteries. Our exploration found that fabricating suitable interface could be most effective way to realize the life stability of SiNWs. The building of silicon homo-structural interface between assembled SiNWs and metallic substrates results in ultra long life for SiNWs, whose capacity is up to 2447mAh g<sup>-1</sup> even after 100 cycles, retaining 80.92% of its second discharge capacity.

## Experimental section

Stainless steel was cleaned thoroughly by ultrasonic vibration in acetone, alcohol and 1wt% H<sub>2</sub>SO<sub>4</sub> solvent orderly for 10min respectively, followed by washing in distilled water till pH value was about 7. The preparation process for SiNWs was shown in figure 1. Silicon and Au layers were evaporated onto the surface of stainless steel orderly by E-beam with a thickness of 20 angstroms and 100 angstroms, respectively (seen in figure 1). The stainless steel substrate deposited with Si-Au bi-layer film was placed in a tubular furnace and then the furnace was heated up to 600 °C with a continuous flow of pure H<sub>2</sub> for three hours. Then the substrate was cooled to room temperature in the furnace with H<sub>2</sub> flow as the protective gas. The surface color of the stainless steel became into light brown after heat-treatment in comparison with the golden color before heat-treatment, and then the stainless steel was cut into circle discs with a diameter of 15mm to be used as the substrate for SiNW growth. SiNW was prepared at 550 °C for 20min with 10% SiH<sub>4</sub> as Si source gas balanced by hydrogen in tubular furnace.

X-ray photoelectron spectroscopy (XPS) measurements were conducted with a K-Alpha 1063 system (Thermo Fisher Scientific) with a monochromatic aluminum K $\alpha$  source and a source power

of 200W. Scanning Electronic Microscope (SEM) images were obtained with Hitachi 4700 FESEM system (Hitachi, Japan).

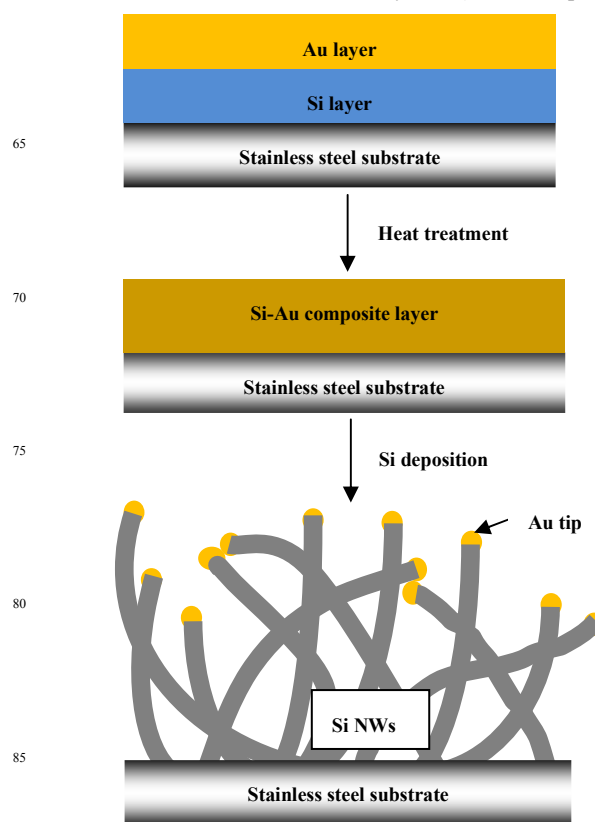


Figure 1. The schematic for SiNW s' preparation process

The electrochemical performance of the SiNWs was tested in 2025 coin cells, in which the deposited SiNWs was used as the working electrode and Li foil acted as counter-electrodes. 1M LiPF<sub>6</sub>/EC+DMC (1:1 in volume) solution was applied as the electrolyte. The electrochemical behavior of the cells was investigated at constant current charging-discharging measurement within the stable voltage window of 0.02V-1.5V. The cyclic voltammogram for the half cell of SiNWs was performed between 0.02V and 2.0V at a scan rate of 0.05mV/s. Electrochemical impedance measurement was performed in the frequency range of 1Hz-0.1MHz with CHI660C (Chenhua Co., China).

## Results and discussion

As illustrated in Figure 1, Au and Si layers were deposited on cleaned stainless steel substrate orderly, and then the substrate was heat-treated to trigger the inter-diffusion of Si and Au layers so as to get Si-rich Au composite catalyst layer. The Si-rich Au composite plays a very important role in the formation of silicon interface layer. Different from Au-catalyzed VLS process, where SiNWs grow directly on its substrates, in our Si-rich Au composite catalyzed process, a very thin silicon film could be formed on the stainless steel substrate preferably earlier than the growth of SiNWs, according to Si-Au binary phase diagram. Therefore, the SiNWs was subsequently grown on the pre-formed silicon film during assembling process. Although this process didn't increase the essential contacting area of SiNWs on

substrate, silicon film between SiNWs and substrate acts as transition layer between them, which not only increases the intrinsic contact area on substrate, but also alleviate the lattice mismatch between SiNWs and their substrates. It is rational to derive that the mechanical stability between stainless steel substrates and SiNWs is increased correspondingly because the contact mode was converted from between SiNWs and stainless steel substrate to between Si film and stainless steel substrate, and the lattice mismatch was avoided technically. In additional, the diameter of SiNWs could be also controlled well by nonequilibrium Si-Au alloying process based on the nonquilibrium heating-cooling process, in which Si-Au alloy and Au particles were formed and precipitated with controllable size.

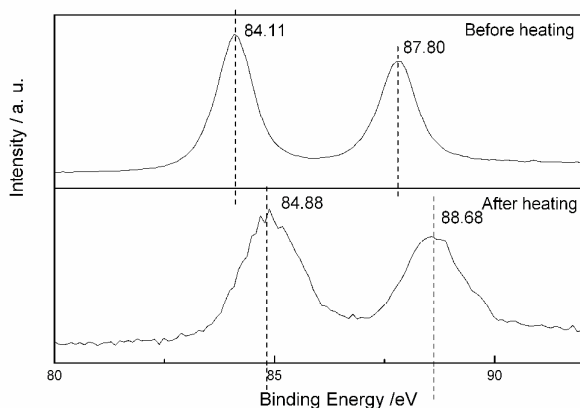
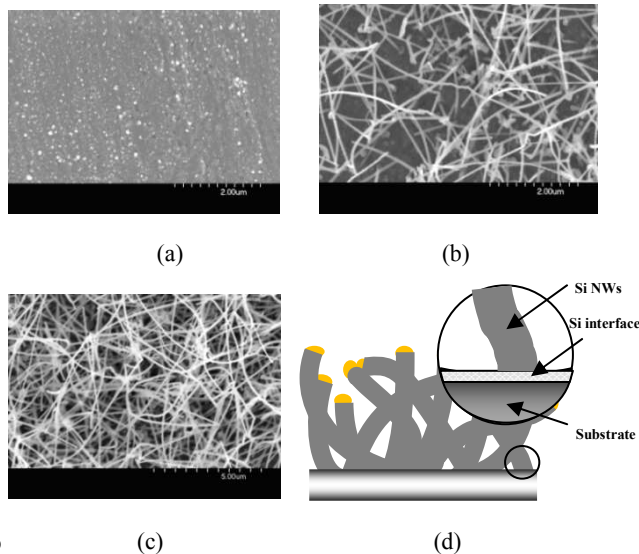


Figure 2. XPS spectra of Au 4f on the surface of stainless steel substrate coated with Si-Au layers before and after heat treatment



The SEM images of the substrate before and after SiNW deposition with different growth time. (a) The morphology of the surface of Si-Au layer coated stainless steel after heat-treatment. (b,c) The image of Si-Au catalyzed SiNWs produced with a deposition time of 10min and 20min respectively. (d) Schematic illustration of the interface between Si-Au catalyzed SiNWs and stainless steel substrate.

The saturated atomic percent of silicon in Si-Au eutectic is 18.6% at 363 K, according to the triple phase point on Si-Au binary phase diagram. In our case, one layer of Si and one layer of Au were pre-deposited on stainless steel substrate respectively before heat treatment. According to our experimental data, the calculated mol ratio of silicon/Au is about 15 % in pre-deposited layer on the presumption of free of holes in the compact layers. Therefore, it is possible to get Si-rich Au composite layer consisting of Au primary crystal and Si-Au eutectic alloy via nonequilibrium heating-cooling process. Figure 2 shows the binding energy changes of substrates coated with Si and Au layers before and after heat treatment. Chemical shift occurred after heat treatment, and the binding energy at 84.88eV represents the existence of Si-Au eutectic alloy after heat treatment.

It is necessary to elucidate why we chose the heated substrates coated with Si-Au layers at the start of SiNW growth rather than Si-Au coated substrates without any further heat treatment. In our previous study, we found the diameter distribution of produced SiNWs could not be controlled well when using Au-coated stainless steel substrates directly because the size of formed Si-Au eutectic droplets was uncontrollable because of the merging behavior of these Si-saturated Au droplets and the different deposition rate of silicon at different location on substrates. So how to control the distribution range of the final diameter of produced SiNWs by a facile way is challengeable. Generally, the diameter size of the prepared SiNW is determined definitely by the initial particle size of catalysts. One optional approach to control the diameter size of SiNWs is to make the catalyst layer by E-beam nanolithography with pre-designed nanopatterns consistent with the final diameter of SiNW. But E-beam nanolithography is a long, very expensive and delicate process, and too many steps are involved to obtain defined Au nanopatterns.

In our typical process in this paper, Si-Au layer coated stainless steel substrates were heated to 600 K and kept for 3 hours to make Si and Au atoms diffuse thoroughly so as to form Si-Au eutectic composite, and then the substrates were cooled with oven under H<sub>2</sub> atmosphere at a high cooling rate. In this nonequilibrium process, the formed Si-Au eutectic would keep its highly Si-Au mixed state, and highly dispersed primary Si-Au alloy particles can thus be remained at a Si-rich state. This nonequilibrium Si-rich Au composite acted as the initial catalysts for the subsequent SiNW growth. Scattered dots were observed on the surface of Si-Au coated substrates after heat-treatment (as seen in figure 3a). During the process of SiNW growth, actually the nonequilibrium catalyst layer was experienced the process of re-precipitation and re-crystallization. The composition of Si-rich Au composite would change with the decomposition of Si gas source, which saturated the Si-Au eutectic all the time, so Si in the Si-Au alloy would be precipitated preferably before the growth of SiNWs. This preferable precipitation process could be demonstrated by an interesting phenomenon that the surface of the substrates was in blue color when the deposited SiNWs were removed off by our moderate scratch, and XPS results also proved that the blue surface is Si film. That is, a very thin transition layer of silicon was actually formed between the prepared SiNWs and stainless steel substrates during SiNW depositing. The existence of this silicon layer could



definitely alleviate the lattice mismatch between SiNWs and metallic substrates. It is understandable that better interface affinity between subsequently produced SiNWs and pre-deposited Si thin film could be gained (schemed in figure 3d).

Figure 3b and Figure 3c exhibit the morphological changes of SiNWs with different growth time. Before SiNW growth, there is some fine particles dispersed on the surface of the stainless steel. After 20-minute SiNW growth (seen in figure 3c), SiNWs could be obviously detected on the substrate with uniform diameter between 100 and 120nm, demonstrating the feasibility of this predeposition-heat-treatment-VLS combined method to control the diameter distribution of final SiNWs. In the following part, SiNWs prepared by this process was designated as Si-Au catalyzed SiNWs.

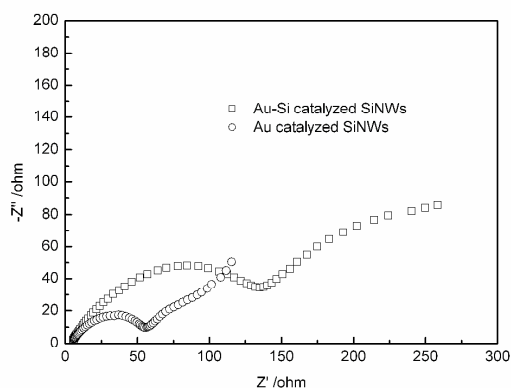


Figure 4. Electrochemical impedance spectrums of silicon nanowires prepared with different catalysts

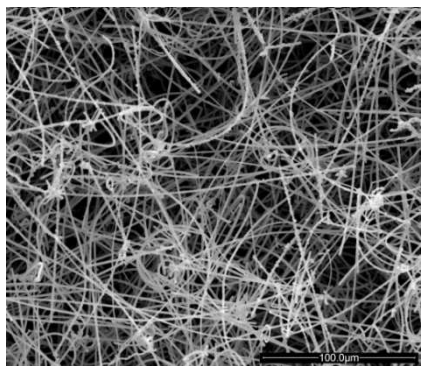


Figure 5. The morphology of Au catalyzed SiNWs

SiNWs catalyzed by pure Au with the same preparation process was also produced in comparison with Si-Au catalyzed SiNWs. SiNWs produced from Au catalyst was designated as Au-catalyzed SiNWs. The impedance comparison of SiNW electrodes from different catalysts is shown in Figure 4. The total impedance of the cell composed of Si-Au catalyzed SiNWs and Li foil is about 134.8ohms with the specific area impedance of  $76.3\text{ohm cm}^{-2}$ , much higher than the impedance of Au catalyzed SiNWs with 61.9ohms. It is worth noting that the impedance actually consists of the impedance of the solid-liquid interfaces between the SiNWs and the electrolyte, the SiNWs and the Si transition film, the Si transition film and the substrate. Although it is very hard to figure out the impedance of silicon transition interface, however, the mass load of these two samples was

controlled almost the same, and the difference between them is mainly from catalyst precursors, so it could be understandable the increment in electrochemical resistance be caused by the precipitated silicon transition layer between substrates and SiNWs during SiNW growth, which could definitely increase the overall resistance of the electrode due to semiconductivity property of silicon. The circuit mode should be researched further to understand the intrinsic electrochemical behavior of this Si-Au catalyzed SiNWs.

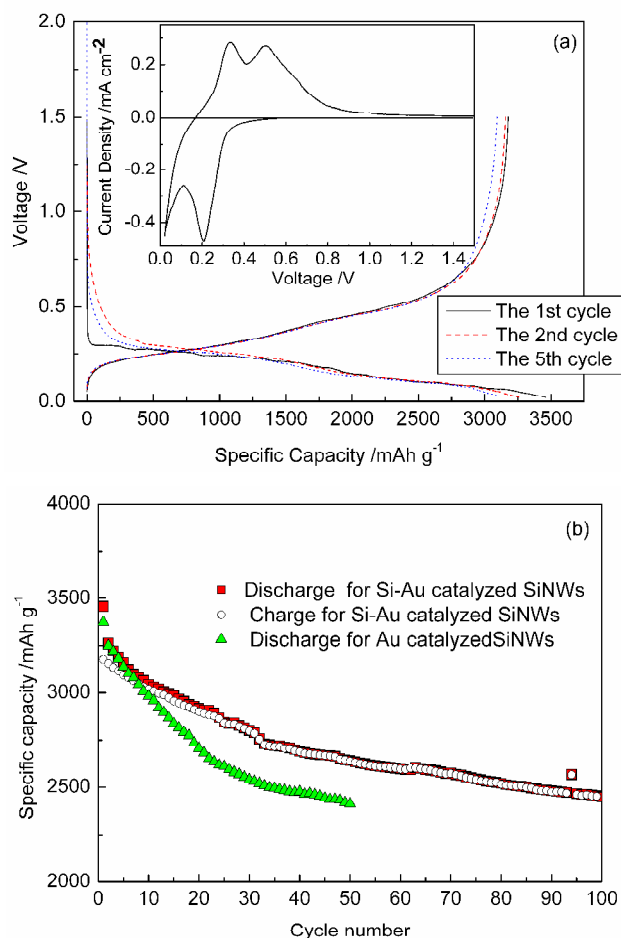


Figure 6. The electrochemical cycling performance of SiNWs: a) The charging-discharging profiles of Si-Au catalyzed SiNWs; b) The comparison of electrochemical cyclability of SiNW electrode produced from different catalysts

Although with larger resistance, the electrochemical performance of Si-Au catalyzed SiNWs from alloyed catalyst shows higher reversibility, comparing with that of Au catalyzed SiNWs. The coulombic efficiency for the first cycle for SiNW electrode from Si-Au catalyst is up to 91.91% (seen in Figure 6a) with a discharge capacity of  $3457.6\text{mAh g}^{-1}$  and a charge capacity of  $3177.8\text{mAh g}^{-1}$ , demonstrating the high reversibility for lithium insertion-extraction. It is interesting to note that there is no obvious behaviour of the formation of solid electrolyte interface (SEI) film taken place during lithium ion insertion for the first cycle, similar to the previous reported.<sup>4, 5, 10, 11</sup> This is

probably another reason for high reversibility in the first cycle. The inset profile is the cyclic voltammogram profile of the as-prepared SiNW electrode for the first cycle. The behavior of Si-Au catalyzed SiNW electrode is similar to the previous reported,<sup>4,5,13,14</sup> There is no SEI formation peak observed on the cathodic curves, especially in the first cycle, consistent with the results of galvanostatic charging-discharging test. The cathodic peaks appearing at 0.18V and 0.02V represent the formation of lithium silicide with different mol ratio of Li/Si, mostly  $\text{Li}_{12}\text{Si}_7$  and  $\text{Li}_{22}\text{Si}_5$ .<sup>3,13</sup> Two corresponding anodic peaks appeared at 0.34V and 0.51V respectively.

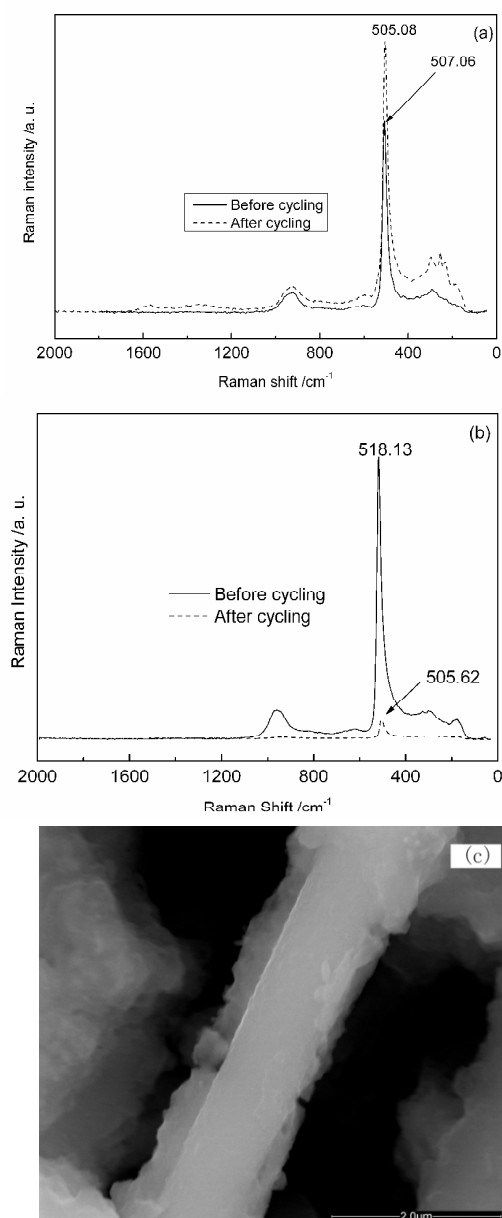


Figure 7. (a) Raman shift of Si-Au catalyzed SiNWs before and after cycling; (b) Raman shift of Au catalyzed SiNWs before and after cycling; (c) SEM image of Si-Au catalyzed SiNWs after cycling

The cycling performance of the Si-Au eutectic catalyzed SiNWs was also investigated, and the comparative cyclability of Si-Au catalyzed SiNWs and Au catalyzed SiNWs is shown in Figure 6b. Very excellent cycling performance of Si-Au catalyzed SiNWs was gained. The cycling performance and reversibility of Si-Au catalyzed SiNWs presents much better than that of Au-catalyzed SiNWs. The retention specific capacity of Si-Au catalyzed SiNWs is up to 80.92% of its second discharge capacity after 100 cycles, whereas that of Au catalyzed SiNWs is only 2539.6 mAh  $\text{g}^{-1}$ , 74.2% after 50 cycles although the deposition process is controlled same. The above part already shows that there is a very thin transition layer of silicon film existing between the produced SiNWs and the stainless steel substrate. Therefore, it could be deduced that although there is some increment in impedance because of the existence of silicon transition layer, however, this thin silicon transition layer make the lattice between SiNWs and substrate match better, which is the main reason of the dramatically increased cycling stability.

As shown in the Raman profiles of Si-Au catalyzed SiNWs before cycling in Figure 7a, there is a strong peak at Raman shift of 507.6  $\text{cm}^{-1}$  rather than at the characteristic Raman shift of 521  $\text{cm}^{-1}$  for the bulk cubic crystalline silicon, presenting Wurtzite nanocrystalline structure in as-prepared Si NWs, which shifts to 505.08  $\text{cm}^{-1}$  after cycling, presenting the crystal changing tendency toward amorphous structure. The tendency on the structure changes of Au-catalyzed SiNWs is almost as the same as that of the Si-Au catalyzed SiNWs before and after cycling. However, the characteristic Raman shift for Au catalyzed SiNWs at 518.13  $\text{cm}^{-1}$  presents more crystallization, which is much closer to the shift of bulk crystalline silicon (Figure 7b). After lithium insertion-extraction, the Au catalyzed SiNWs changes into amorphous, resulting in the Raman shift at 505.62  $\text{cm}^{-1}$ , but the relative intensity became very weak, due to the serious peeling off of SiNWs from the substrate. The peeling off phenomenon wasn't detected on the Si-Au catalyzed SiNWs' electrode. This is probably due to the stability of silicon interface between the SiNWs and the substrate. In addition, the irreversibility in structure would trap more lithium ions in the defects occurring in the course of electrochemical lithium insertion-extraction, so the difference in the start crystallization of SiNWs from different catalysts shows different cycling capability. Figure 6c presents the morphology of the Si-Au catalyzed SiNWs after cycling. The surface of the SiNWs becomes very coarse for the formation of SEI film, but there is no obvious defects embedded on the nanowires (Figure 7c).

## Conclusions

In conclusion, the present work demonstrates a new and facile approach based on interface enhancement to fabricating a long life SiNWs with a simply modified Si-rich Au composite as the catalyst. The utilization of this Si-rich Au catalyst can induce the formation of Si transition layer between as-deposited SiNWs and the stainless steel substrates, which not only improves the lattice match between them, but also increases the contact area of Si active center with the substrates by converting the interface contact from point contact between SiNWs and stainless steel substrate to planar contact between Si film and stainless steel substrate. The electrochemical performance could thus be

enhanced dramatically. Structuring homo-structural interface offers a promising strategy by interface modification to alleviate the irreversibility of silicon or other high capacity anode materials.

## 5 Acknowledgements

This research is financially supported by the Natural Science Foundation of China (Grant No. 21476035), the Fundamental Research Funds for the Central Universities (Grant No. 3132014077 and Grant No. 3132014323), the Research Funds of Education Department of Liaoning Province (Grant No. L2013204), and the Natural Science Foundation of Liaoning Province (Grant No. 2014025016).

## Notes and references

<sup>a</sup> Institute of Materials and Technology, Dalian Maritime University,  
15 Dalian 116026, China. Fax: 86-411-84729611; Tel: 86-411-84727971;  
E-mail: zswen5@gmail.com

1. L. Ji, M. Rao, S. Aloni, L. Wang, E. J. Cairns, and Y. Zhang, *Energy Environ. Sci.*, 2011, **4**, 5053; E. Eustache, P. Tilmant, L. Morgenroth, P. Roussel, G. Patriarche, D. Troadec, N. Rolland, T. Brousse and C. Lethien, *Adv. Energy Mater.*, 2014, **4**, 1301612; B. Guo, X. Yu, X.-G. Sun, M. Chi, Z. -A. Qiao, J. Liu, Y. -S. Hu, X. -Q. Yang, J. B. Goodenough and S. Dai, *Energy Environ. Sci.*, 2014, **7**, 2220; L. Ji, Z. Tan, T. R. Kuykendall, E. J. An, Y. Fu, V. Battaglia and Y. Zhang, *Energy Environ. Sci.*, 2013, **4**, 3611; J. Hwang, S. H. Woo, J. Shim, C. Jo, K. T. Lee and J. Lee, *ACS Nano*, 2013, **7**, 1036; Y. J. Kim, H. Lee, H. J. Sohn, *Electrochem. Commun.*, 2009, **11**, 2125.
2. D. Larcher, G. Sudant, J.-B. Leriche, Y. Chabre and J.-M. Tarascon, *J. Electrochem. Soc.*, 2002, **149**, A234.
3. J. Graetz, C. C. Ahn, R. Yazami and B. Fultz, *Electrochem. Solid-State Lett.*, 2003, **6-9**, A194; D. Larcher, S. Beattie, M. Morcrette, K. Edstrom, J. -C. Jumas and J. -M. Tarascon, *Mater. Chem.*, 2007, **17**, 3759; M. N. Obrovac and L. J. Krause, *J. Electrochem. Soc.*, 2007, **154**, A103.
4. C. K. Chani, H. Peng, G. Liu, K. Mcilwrath, X. F. Zhang, R. A. Huggins and Y. Cui, *Nat. Nanotech.*, 2008, **3**, 31.
5. M. -H. Park, M. G. Kim, J. Joo, K. Kim, J. Kim, S. Ahn, Y. Cui and J. Cho, *Nano Lett.*, 2009, **9**, 3844; C. K. Chan, R. Ruffo, S. S. Hong, R. A. Huggins and Y. Cui, *J. Power Sources*, 2009, **189**, 34; V. Schmidt, J. V. Wittemann, S. Senz and U. Gösele, *Adv. Mater.*, 2009, **21**, 268; K. Peng, J. Jie, W. Zhang and S. -T. Lee, *Appl. Phys. Lett.*, 2008, **93**, 033105; H. Wu, G. Chan, J. W. Choi, I. Ryu, Y. Yao, M. T. McDowell, S. W. Lee, A. Jackson, Y. Yang, L. Hu and Y. Cui, *Nat. Nanotech.*, 2013, **7**, 310; V. Chakrapani, F. Rusli, M. A. Filler and P. A. Kohl, *J. Power Sources*, 2012, **205**, 433.
6. H. T. Nguyen, F. Yao, M. R. Zamfir, C. Biswas, K. P. So, Y. H. Lee, S. M. Kim, S. N. Cha, J. M. Kim and D. Pribat, *Adv. Energy Mater.*, 2011, **1**, 1154.
7. V. A. Nebol'sin and A. A. Shchetinin, *Inorg. Mater.*, 2003, **39**, 899.
8. H. -Y. Tsao and Y. -J. Lin, *Appl. Phys. Lett.*, 2014, **104**, 053501; V. A. Nebol'sin, A. A. Shchetinin, A. A. Dolgachev and V. V. Korneeva, *Inorg. Mater.*, 2005, **41**, 1256; B. M. Kayes, M. A. Filler, M. C. Putnam, M. D. Kelzenberg, N. S. Lewis and H. A. Atwater, *Appl. Phys. Lett.*, 2007, **91**, 103110.
9. N. Shin and M. A. Filler, *Nano Lett.*, 2012, **12**, 2865.
10. J. R. Maiolo, B. M. Kayes, M. A. Filler, M. C. Putnam, M. D. Kelzenberg, H. A. Atwater and N. S. Lewis, *J. Am. Chem. Soc.*, 2007, **129**, 12346.
11. N. Dimov, S. Kugino, M. Yoshio, *Electrochim. Acta.* 48 (2003) 1579-1583.
12. Z. Wen, J. Yang, B. F. Wang, K. Wang and Y. Liu, *Electrochem. Commun.*, 2003, **5**, 165; J. Shu, H. Li, R. Yang, Y. Shi and X. Huang, *Electrochem. Commun.*, 2006, **8**, 51; A. Magasinski, P. Dixon, B. Hertzberg, A. Kvit, J. Ayala and G. Yushin, *Nat. Mater.*, 2010, **9**, 353; J. P. Maranchi, A. F. Hepp and P. N. Kumta, *Electrochem. Solid-State Lett.*, 2003, **6**, A198; H. Jung, M. Park, S. H. Han, H. Lim, S.-K. Joo, *Solid State Commu.*, 2003, **125**, 387.
13. Z. S. Wen, J. Stark, R. Saha, J. Parker and P. A. Kohl, *J. Phys. Chem. C*, 2013, **117**, 8604.
14. Z. S. Wen, M. K. Cheng, J. Sun and L. Wang, *Electrochimica Acta*, 2010, **56**, 372.
15. S. W. Kim, J. H. Yun, B. Son, Y. -G. Lee, K. M. Kim, Y. M. L, and K. Y. Cho, *Adv. Mater.*, 2014, **26**, 2977; H. Kim and J. Cho, *Nano. Lett.*, 2008, **8**, 3688; B. Hertzberg, A. Alexeev and G. Yushin, *J. Am. Chem. Soc.*, 2010, **132**, 8548.
16. L. Ji, H. Zheng, A. Ismach, Z. Tan, S. Xun, E. Lin, V. Battaglia, V. Srinivasan and Y. Zhang, *Nano Energy*, 2012, **1**, 164.
17. C. Yu, X. Li, T. Ma, J. Rong, R. Zhang, J. Shaffer, Y. An, Q. Liu, B. Wei and H. Jiang, *Adv. Mater.*, 2012, **2**, 68.
18. D. Munaò, M. Valvo, J. v. Erven, E. M. Kelder, J. Hassoun and S. Panero, *J. Mater. Chem.*, 2012, **22**, 1556.

**A novel approach to getting long cycle life for silicon nanowires via homostructured interface from nonequilibrium Si-Au catalysts is proposed.**

